Analysis of RPE morphometry in human eyes

Shagun K. Bhatia,[1] Alia Rashid,[1] Micah A. Chrenek,[1] Qing Zhang,[1] Beau B. Bruce,[1,2,3] Mitchel Klein,[2,4] Jeffrey H. Boatright,[1,5] Yi Jiang,[6] Hans E. Grossniklaus,[1] John M. Nickerson[1]

[1]Department of Ophthalmology, School of Medicine, School of Medicine, Emory University, Atlanta, GA; [2]Department of Epidemiology, Rollins School of Public Health, Emory University, Atlanta, GA; [3]Department of Neurology, School of Medicine, Emory University, Atlanta, GA; [4]Department of Environmental Health, Rollins School of Public Health, Emory University, Atlanta, GA; [5]Center for Visual and Neurocognitive Rehabilitation, Atlanta VA Medical Center, Decatur, GA; [6]Department of Mathematics and Statistics, Georgia State University, Atlanta, GA

Purpose: To describe the RPE morphometry of healthy human eyes regarding age and topographic location using modern computational methods with high accuracy and objectivity. We tested whether there were regional and age-related differences in RPE cell area and shape.

Methods: Human cadaver donor eyes of varying ages were dissected, and the RPE flatmounts were immunostained for F-actin with AF635-phalloidin, nuclei stained with propidium iodide, and imaged with confocal microscopy. Image analysis was performed using ImageJ (NIH) and CellProfiler software. Quantitative parameters, including cell density, cell area, polygonality of cells, number of neighboring cells, and measures of cell shape, were obtained from these analyses to characterize individual and groups of RPE cells. Measurements were taken from selected areas spanning the length of the temporal retina through the macula and the mid-periphery to the far periphery.

Results: Nineteen eyes from 14 Caucasian donors of varying ages ranging from 29 to 80 years were used. Along a horizontal nasal to temporal meridian, there were differences in several cell shape and size characteristics. Generally, the cell area and shape was relatively constant and regular except in the far periphery. In the outer third of the retina, the cell area and shape differed from the inner two-thirds statistically significantly. In the macula and the far periphery, an overall decreasing trend in RPE cell density, percent hexagonal cells, and form factor was observed with increasing age. We also found a trend toward increasing cell area and eccentricity with age in the macula and the far periphery. When individuals were divided into two age groups, <60 years and ≥60 years, there was a higher cell density, lower cell area, lower eccentricity, and higher form factor in the younger group in the macula and the far periphery ($p<0.05$ for all measurements). No statistically significant differences in RPE morphometry between age groups were found in the mid-periphery.

Conclusions: Human cadaver RPE cells differ mainly in area and shape in the outer one third compared to the inner two-thirds of the temporal retina. RPE cells become less dense and larger, lose their typical hexagonal shape, and become more oval with increasing age.

The RPE is located in between the neurosensory retina and the choroid. The main functions of the RPE are to supply the highly metabolically active retina with nutrients and remove waste by-products from the photosensory processes of the cones and rods. The RPE plays a key role in the pathogenesis of age-related macular degeneration (AMD) [1,2]. The healthy structure of the RPE sheet has been described as a monolayer of homogeneous cells of hexagonal shape, forming a barrier between the neurosensory retina and the underlying choriocapillaris [3]. This honeycomb appearance of the RPE is known to be the most stable configuration of cells of the same size in nature [4]. A hexagonal network of cells allows for the greatest coverage of area without cell overlap or empty areas and with the least amount of surface tension [4]. Little

is known about how the morphometry of RPE cells changes with location or normal aging. Understanding the normal aging process of RPE will help us better understand differences in age-related retinal pathology.

Age-related loss of RPE cells has been reported in previous literature using various methods (Table 1). A prior study by Panda-Jonas et al. [5] reported a 0.3% decrease per year, and Del Priore et al. [6] found a 0.23% rate of decline per year. In contrast, other investigators, such as Watzke et al. [7] and Harman et al. [8], found no age-dependent changes in RPE cell density. Previous studies by Ts'o and Friedman [9], and Dorey et al. [10], which looked at different retinal regions, showed that RPE cell density in the macula decreases with age. Gao and Hollyfield [11] concluded that the RPE declines at a rate of 14 RPE cells/mm^2 per year.

Investigators have also described changes in RPE cell density in relation to location in the retina. Several studies have shown that RPE cell density decreases with increasing

Correspondence to: John M. Nickerson, Department of Ophthalmology, Room B5602, Emory University, 1365B Clifton Road, NE, Atlanta, GA 30322; Phone: (404) 778-4411; FAX: (404) 778-2231; email: litjn@emory.edu

TABLE 1. SUMMARY OF PAST STUDIES.

Study Authors	Sample Size	Cells	Areas of Retina	Measurements	Methods	Study Findings
Ts'o and Friedman [9]	10 eyes	RPE	5 concentric regions around the macula	Cell density Cell area	RPE flatmounts were bleached; cells counted manually; cell area determined by dividing the total retinal area by # of cells	- RPE cell density decreases in the posterior pole with age - equatorial RPE cell density increased with age cell area decreased with age in posterior pole, increased in equator and periphery
Dorey et al. [10]	30 eyes	PF RPE	Macula Paramacula Equatorial	Cell density	Fixed and embedded eyes; cells counted manually from radial sections	- RPE density decreased in posterior pole; not quantified - No changes with age in equator
Gao and Hollyfield [11]	35 eyes	GC** PR RPE	Fovea Peripheral Retina	Cell Density	Tissue was embedded and sectioned; cells counted by one observer	- No age related changes in foveal RPE cell density - Peripheral RPE loss 14 cells/mm²/year - RPE density=5531 - 14 X age (years), Foveal RPE density 63% higher than periphery
Watzke et al. [7]	20 eyes	RPE	Fovea Temporal Posterior pole Peripheral retina	Cell density Cell area Form factor Polymegathism	RPE flatmounts were bleached; cells counted manually	- no age effect on cell density or cell area found in any of the regions - RPE cells of fovea and temporal posterior pole were more hexagonal in younger eyes
Panda-Jonas et al. [5]	53 eyes	PR* RPE	Fovea Mid-periphery Outer-periphery	Cell Density	25 biopsy specimens of the retina and RPE; Cells were counted from photographs	- Total RPE cell density decreased by 0.3% per year - fovea (4,220±727 cells/mm²) - mid-periphery (3,002±460 cells/mm²) - outer periphery (1,600±411 cells/mm²)
Harman et al. [8]	38 eyes	RPE	Whole Retina	Cell Density	Whole-mounted RPE; cells counted by manual tracing	- No age effect on cell density found in any regions of retina
Del Priore et al. [6]	22 eyes	RPE	4 concentric regions around the fovea	Cell Density # Apoptotic cells	RPE flatmounts were TUNEL stained and counted	- Total RPE cell density decreased by 0.23% per year - RPE density (cells/mm²)=4,890×11.3 (age) - Significant change in the density of RPE cells only seen in Zone 4 - Cell density decreased in the RPE w/increased distance from fovea - Zone 1 (4980±90 cells/mm²); Zone 2 (4857±75 cells/mm²)' Zone 3 (4068±207 cells/mm²); Zone 4 (4024±137 cells/mm²)

*PR=Photoreceptors; **GC=Ganglion Cells; RPE=Retinal Pigment Epithelium; TUNEL=Terminal deoxynucleotidyl transferase dUTP nick end labeling

distance from the optic nerve [5,6,11]. Gao and Hollyfield [11] found foveal RPE cell density to be 63% higher than at the periphery. Panda-Jonas et al. [5] and Del Priore et al. [6] also quantified RPE cell density in various areas of the retina. Del Priore et al. [6] found macular RPE cell density to be 4,980±90 cells/mm^2.

Currently, the RPE can be imaged in vivo with adaptive optics scanning laser ophthalmoscopy (AOSLO), an imaging technique used to measure living retinal cells [12]. Preliminary studies showed the instrument's ability to image individual photoreceptor and RPE cells in humans and rhesus macaques [13,14], allowing for quantitative measurements of these retinal cells. Similar research on the cornea has allowed for morphometric measurements of corneal endothelial cells, which are now used for the clinical diagnosis of corneal pathology using specular microscopy [15].

We hypothesize that with increasing distance from the optic nerve and with increasing age, the RPE will become increasingly disorganized. In this study, we describe normal changes in RPE morphometry that occur with location and age, establishing a baseline, which can be used to detect individuals who are outside the normal range. We aim to 1) estimate associations that exist between measures of RPE morphometry, including cell density, cell area, eccentricity, form factor, and percent of hexagonal cells, 2) compare RPE morphometry in location and areas of the retina (the macula, through the mid-periphery to the far periphery), and 3) describe the association between age and measures of RPE morphometry, which might predict "RPE age" using data acquired from this study.

This study provides morphometric measurements that may be translatable to the clinical setting when combined with clinical imaging modalities. We expected that with age, RPE cells would become increasingly disorganized, with changes also dependent on the geographic zone.

METHODS

Eye tissue: The Emory University Institutional Review Board (IRB) determined that the present study of deidentified human cadaver eyes had exempt status for IRB approval. The exempt status is in full compliance with and adheres to the tenets of the Declaration of Helsinki and the ARVO statement on human subjects. Nineteen normal human cadaver eye globes or posterior poles from 14 donors of varying ages were obtained from the Georgia Eye Bank (Atlanta, GA) and the North Carolina Eye Bank (Winston-Salem, NC) over a 3-year period from 2011 to 2013. Eyes were considered for analysis if the donors were between the ages of 10 and 90 years old, if there was no documented history of ocular disease, no documented history of inherited or acquired retinal disease, and no apparent signs of chorioretinal pathology at the time of tissue processing. An exception was made for retinal detachment outside the dissected region of interest described in the next paragraph. Eyes with prior cataract surgery or cataractous lenses were not excluded from the study. The donor sample had a fairly even sex distribution, generalizable to most populations of interest. Cancer was the most common cause of death of donors in this study set, not atypical of the U.S. population [16]. In an attempt to avoid samples with tissue degradation, eyes were excluded from the study if the time between the death of the donor and preservation of the globe in fixative was greater than 7 h [17]. The average death to preservation time of less than 7 h ensured that the tissue used in this study had minimal autolytic changes [17,18].

Tissue processing: Eyes were immediately immersed in Z-fix (Anatech Ltd., Battle Creek, MI), a buffered zinc formalin fixative solution, for 24–32 h before being dissected. Whole eyes were dissected by sectioning the globe superiorly and inferiorly to obtain a pupillo-optic (PO) nerve section that included the optic nerve head (ONH) and the macula and extended to the ciliary bodies bilaterally (Figure 1A–F). The neurosensory retina was then carefully separated from the RPE (Figure 1G), leaving the exposed RPE, Bruch's membrane, the choroid, and the sclera (Figure 1H). The RPE, Bruch's membrane, and the choroid were removed from the sclera and flatmounted on a slide with a silicon barrier (Grace Bio-Labs, Bend, OR; Figure 1I).

Orientation of the tissue was maintained and noted. RPE flatmounts were stained with AlexaFluor 635-Phalloidin (Life Technologies, Grand Island, NY) to stain F-actin at the borders of the RPE cells and propidium iodide (Life Technologies, Grand Island, NY) to stain the nuclei. The RPE was then imaged using a Nikon C1 confocal (Nikon, Tokyo, Japan) in a 15 µm thick stack, and flat images were generated using maximum intensity projection using ImageJ [19] with the LOCI Bio-Formats tool [20] (Figure 2A). Multiple images were photomerged using Autopano Pro v2.5 software (Kolor, Montmélian, France) or with Photoshop version 2 (Adobe Systems, Inc., San Jose, CA) to create a composite image. This method of dissection and staining resulted in images in which cell borders and nuclei were identified clearly.

Imaging and data collection: Individual images used for analysis were excluded from this study if they were of low quality (large fluorescent specks, obvious dissection damage, extensive wrinkles due to preparation, faint outlines of cell borders, or high intracellular background). Image analysis was performed using CellProfiler software (Broad Institute, Cambridge, MA) [21]. We assessed the accuracy of
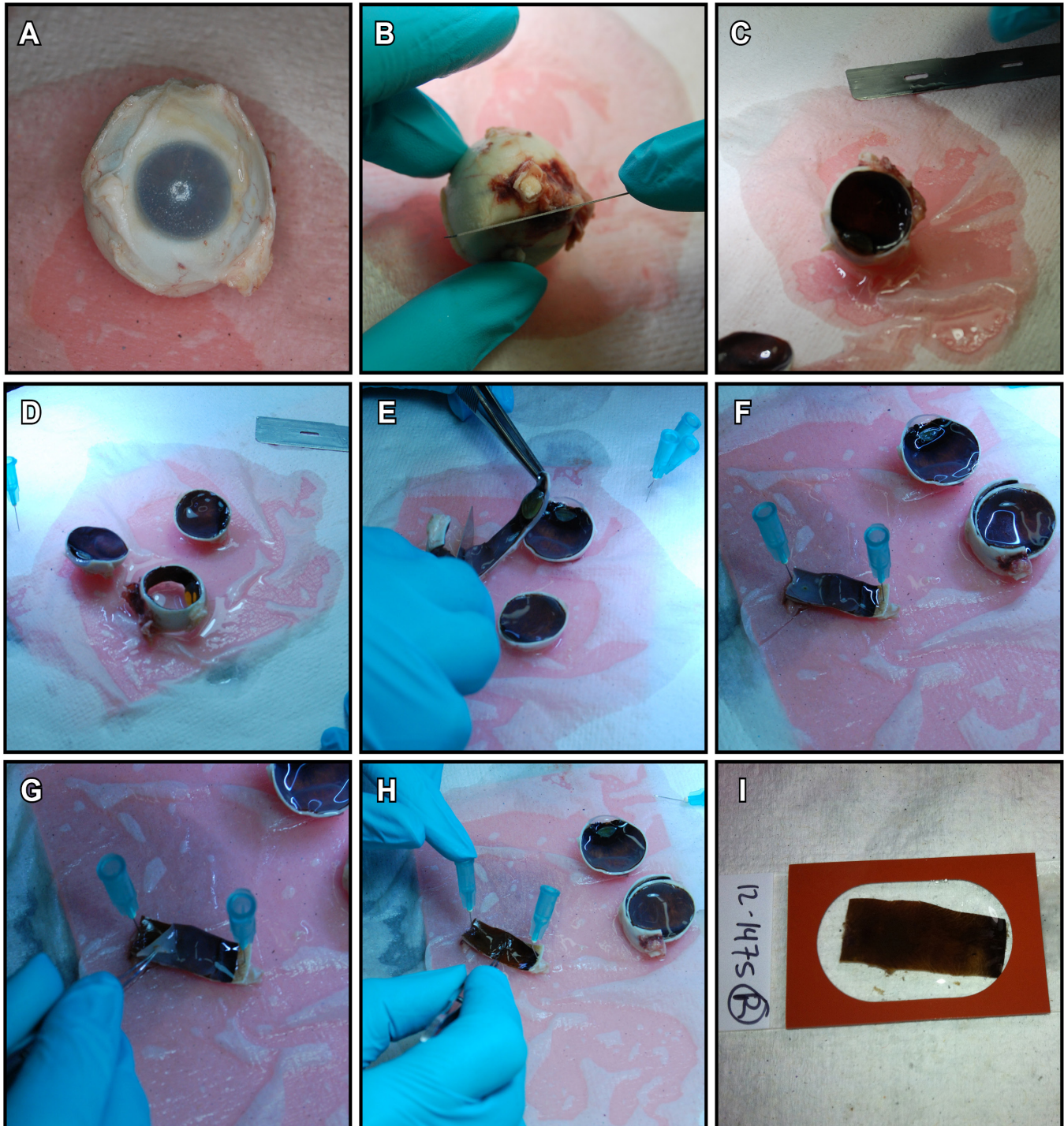
Figure 1. Description of microdissection methods. Whole eyes were received from the eye bank. **A**: Orientation of the eye was identified using the superior and inferior oblique muscle insertions and the long posterior ciliary artery as landmarks. **B**: The superior calotte was removed and dissected approximately 2 mm above the optic nerve and 1 mm into the cornea in the AP section. **C**: The eye with the macula region visible in the cross-section. **D**: The inferior calotte was removed, again approximately 2 mm below the optic nerve and approximately 1 mm into the inferior corneal margin. **E**: The pupillo-optic (PO) section was opened by first cutting the ciliary body tissue adjacent to the lens on the side of the macula and then making the second cut at the optic nerve border. **F**: The cut tissue section was pinned to a paper-covered wax board and trimmed to an appropriate size if necessary. **G**: Using forceps, the retina layer was peeled away from the RPE. **H**: Using closed curved forceps, the RPE/choroidal tissue was separated from the underlying sclera. Microscissors may be required to cut the vascular connections in the macular region. **I**: The RPE/choroidal tissue section was placed on a slide in balanced salt solution (BSS) until ready to stain.
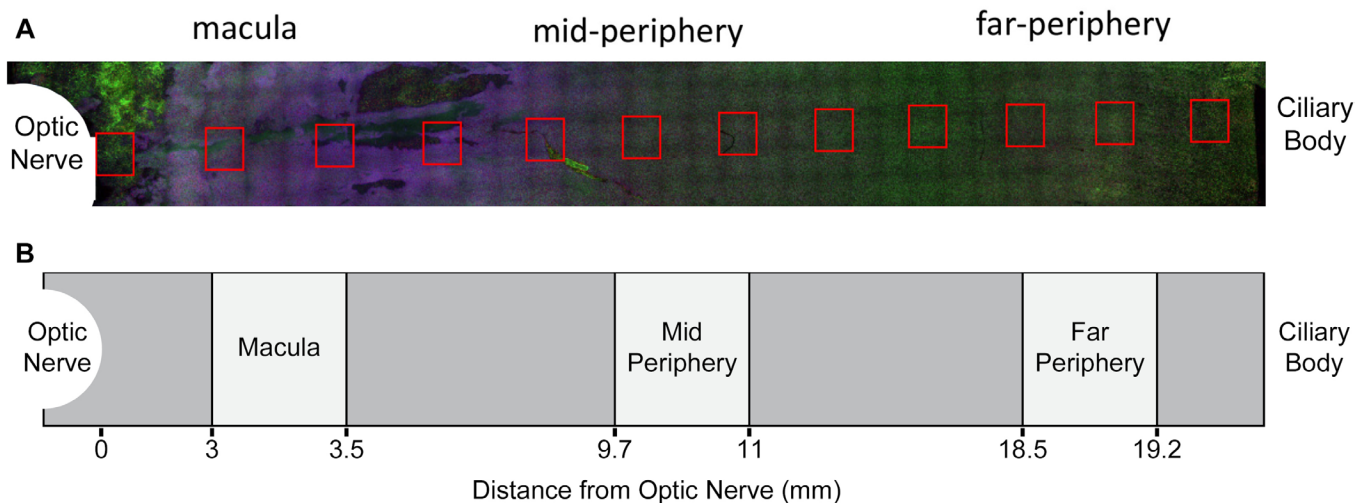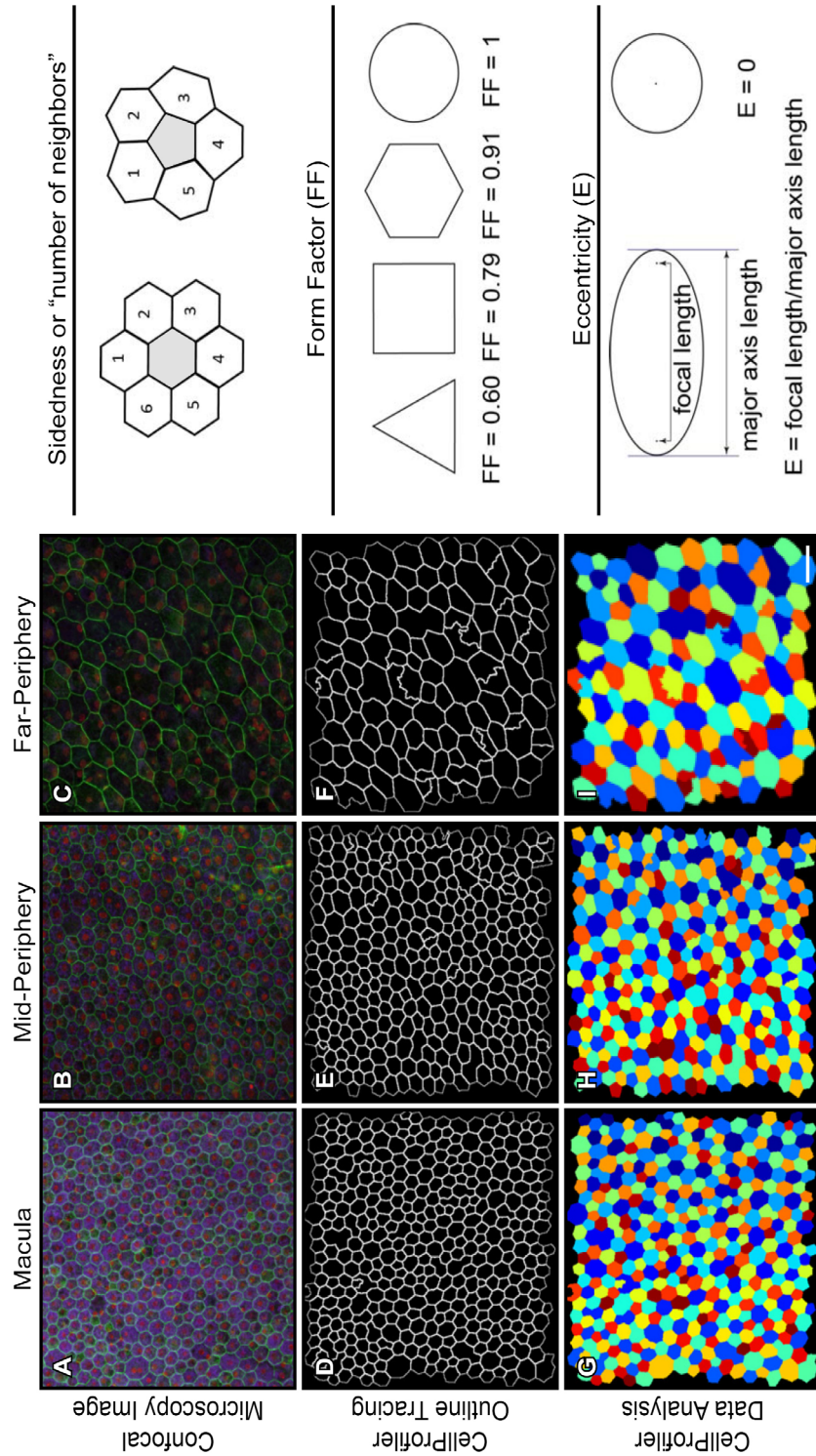
Figure 2. Image Selection criteria for the two studies: the location study and the aging study. **A**: For the location study, we stitched together a strip of images from the optic nerve head (ONH) to the far periphery and analyzed 1,024 × 1,024 pixel images spaced apart by 2,048 pixels. Typically, this gave us 12 images that we analyzed, and these images are marked in this representative strip as red boxes. **B**: For the aging study, a total of nine images were selected for analysis from each donor eye. Three images were selected from each of the above zones. Zone 1 corresponded to the macula, identified as the area 3.0–3.5 mm from the optic nerve and the area of the retina with the highest RPE cell density. Zone 2 corresponded to the mid-periphery, which was measured to be 9.7–11 mm from the optic nerve. Zone 3 corresponded to the far periphery, which was measured to be 18.5 to 19.2 mm from the optic nerve.

CellProfiler by comparing data from hand-traced images to data from CellProfiler. CellProfiler analysis allowed a degree of objectivity when analyzing samples. The software avoided observer bias and introduced error by tracing and analyzed the samples more quickly. There was no difference (not statistically significant; data not shown) between the hand-traced and CellProfiler-traced samples in the present studies with human cadaver eyes and in previous studies with mouse eyes [22-24]. We also demonstrated the integrity of the data from CellProfiler by showing a perfect linear correlation between the reciprocal of the average cell area and the cell density and a strong negative correlation between the average form factor and the average eccentricity.

For location studies, measurements were recorded from 12 images (from one quarter of a 1,024 × 1,024 pixel image) spaced 2048 pixels apart from the optic nerve head to the temporal far periphery (as described in Figure 2A). For aging studies, measurements were taken from three zones spanning the length of the retina, corresponding to the macula, temporal mid-periphery, and temporal far periphery of the retina (Figure 2B). Only the temporal mid-periphery and the temporal far periphery were examined to have a continuous strip of retina that included the optic nerve and the macula while maintaining strict consistency in sampling location between donors. The macula was identified as being 3.0–3.5 mm from the end of the optic nerve, which histologically is correlated to the anatomic fovea [25]. Three images of

512 × 512 pixels were used from each zone for morphometric analysis. Cell borders were automatically traced and analyzed using CellProfiler software (Figure 3) providing several quantitative morphometric measurements. Five morphometric parameters were analyzed in this study: cell density, number of cell neighbors, cell area, eccentricity, and form factor. Eccentricity, a measure of cell shape, provided information about how elongated a cell was (Figure 3). A perfect circle has an eccentricity value of 0, while a highly extended oval has an eccentricity value approaching 1, according to this formula $(a^2 - b^2)^{1/2}$, where a and b represent the semimajor axis and the semiminor axis, respectively, of an ellipse that best fits the polygonal cell shape. An equivalent definition of eccentricity is the ratio of the focal length to the major axis length. Form factor measures the deviation of a cell from the shape of a perfect hexagon, taking into account that not all six-sided cells are equilateral hexagons [26]; see Figure 3. The form factor value is defined as the ratio of the cell's area to the square of the cell's perimeter. A cell that is a perfect equilateral hexagon has a form factor value of about 0.84, while less regularly shaped hexagons have lower values. The analysis technique used in this study objectively measured many more morphometric parameters of the RPE, to characterize individual and groups of RPE cells of different ages and locations.

Statistical analysis: In the text and legends, all metrics are summarized as the mean ± standard deviation. A univariate

Figure 3. Image analysis techniques. **Left**: CellProfiler version 2.1.1 image analysis software was used to automatically trace cell borders from individual images (top, original raw images; middle, traced cell borders; bottom, colored cells were analyzed). Scale bar equals 25 μm. **Right**: Metrics used to evaluate each cell. Top: Sidedness, counting the number of contacting neighbor cells. Middle: Form factor, the relationship of perimeter to area according the definition 4π area/perimeter^2. The form factor value for a perfect equilateral hexagon is 0.84. A decreased form factor value corresponds to a cell with fewer sides or with sides of unequal lengths. Bottom: Eccentricity, a measure of the elongation of a cell approximated by an elliptical shape. Eccentricity is the ratio of the focal length to the major axis length, and a higher value corresponds to a more elongated shape. The right half is taken from Appendix 9 in reference [24] with permission of the authors, according to CCL 3.0 BY-NC-ND.

analysis was performed to provide descriptive statistics for each morphometric measurement. Next, associations between measurements were identified and analyzed using linear regression. To assess for the spatial variation of RPE morphometric measurements between three areas of the retina, a one-way Analysis of Variance (ANOVA) test was performed. Linear regression analysis was used to estimate associations between RPE cell morphology and age in three areas of the retina. From this analysis, we estimated specific rates of changes that occurred with age. We also divided the tissue samples into two groups: less than 60 years of age and greater than or equal to 60 years of age, with 60 the age when retinal pathology such as AMD begins to become more obvious (See Facts about Age-related Macular degeneration. NEI 2009). We then compared measurements between the two age groups with a two-sided Student *t* test. The curves on each panel of Figure 4 were created using the trendline tool in Excel and a second-order polynomial for regression. Each trendline was from all four subjects. One-way ANOVA and Tukey analysis were performed with GraphPad Prism (La Jolla, CA) version 6.1 software. Other analyses were conducted with SAS, version 9.4 (Cary, NC).

RESULTS

Geographic location study: A group of eyes from four donors was used to examine geographic (location) variations in RPE cell characteristics. The ages of the donors were 54, 66, 68, and 71. We used CellProfiler software to avoid potential observer biases. We found that CellProfiler was as accurate and precise as human hand-traced cells and counts in prior studies in mouse RPE [22-24] and here in the initial studies with human cadaver eyes (data not shown). Blocks of about 100 to 300 cells per image appeared adequate based on limited image analyses that compared hand-traced cells versus CellProfiler. We consistently found that strips or blocks taken from the same locations subsampling 100–300 cells out of about 400–1200 cells were adequately representative and were not statistically significantly different. Thus, samples of 100–300 cells were used in further analyses with >100 cells in a cluster as the minimum accepted block for subsequent work. Representative images from the macula, temporal mid-periphery, and temporal far periphery from the confocal microscope (top row) and processed through Cell-Profiler (middle and bottom rows) are shown in Figure 3A.

To adequately sample RPE cells from the ONH to the far periphery, 1,024 × 1,024 pixel images were recorded, then 2048 pixels were skipped, and another 1,024 × 1,024 pixel image was recorded, and so on, until no more RPE could be fully imaged. This typically resulted in 12 images horizontally

(Figure 2A). Images were processed and analyzed in CellProfiler, collecting more than 23 size and shape characteristics for each cell in each image. Here we report on five common parameters: cell density, cell area, eccentricity, form factor, and sidedness, or number of neighbors. Cell density as a function of distance from the ONH is illustrated in Figure 4A. Cell density remained consistent until approximately 13 mm from the ONH (i.e., the far periphery). Cell density at the posterior pole was about four times greater than at the far periphery. Cell area (Figure 4B) showed an inverse correlation to cell density as there were no extracellular spaces, gaps, or atrophy between or among the RPE cells in these "normal" RPE sheets. The cell area remained consistent until approximately 15 mm from the ONH. The mean cell areas at the far periphery were about four times the value at the macula. Form factor decreased from the macula to far periphery, but only by a small amount; the peak form factor values at the macula were 0.74–0.76 (and for comparison, this is less than the form factor of a regular pentagon) and decreased by 12% at the far periphery (Figure 4C). There was a clear trend of increasing eccentricity from the macula toward the far periphery, increasing by 38% (Figure 4D). In Figure 4E, the number of neighbors (sidedness) was highest and most uniform (about 5.7 neighbors per cell) in the macula and the mid-periphery. Only in the far periphery, more than 15 mm from the ONH, did sidedness fall below 5.6 neighbors per cell. In these five metrics, the far periphery was statistically significantly different ($p<0.05$) from the mid-periphery and the macula (see Table 2 , Table 3, Table 4, Table 5, and Table 6 for statistical comparisons).

Aging study: Donor characteristics: A total of ten donors were used in this aging study ranging from 29 to 80 years old, with an average age of 58.8 years. One hundred percent of the donors were Caucasian, and 60% of the donors were male. The most common cause of death was related to various advanced cancers. The death to preservation time was collected for 90% of the donors and ranged from 39 min to almost 7 h, with an average death to preservation time of 4.31 h (Table 7).

Representative images (Figure 5) comparing a younger individual (37 years) to an older individual (75 years) clearly showed changes in RPE morphometry. The older individual displayed a decreased cell density, increased cell area, and loss of the uniform hexagonal epithelium in all three areas of the retina, corresponding to the five morphometric measurements used in the location study. These images also showed increasing cell disorganization and a more irregular cell shape in the young and old individuals with increasing distance from the optic nerve. We observed numerous clusters of cells
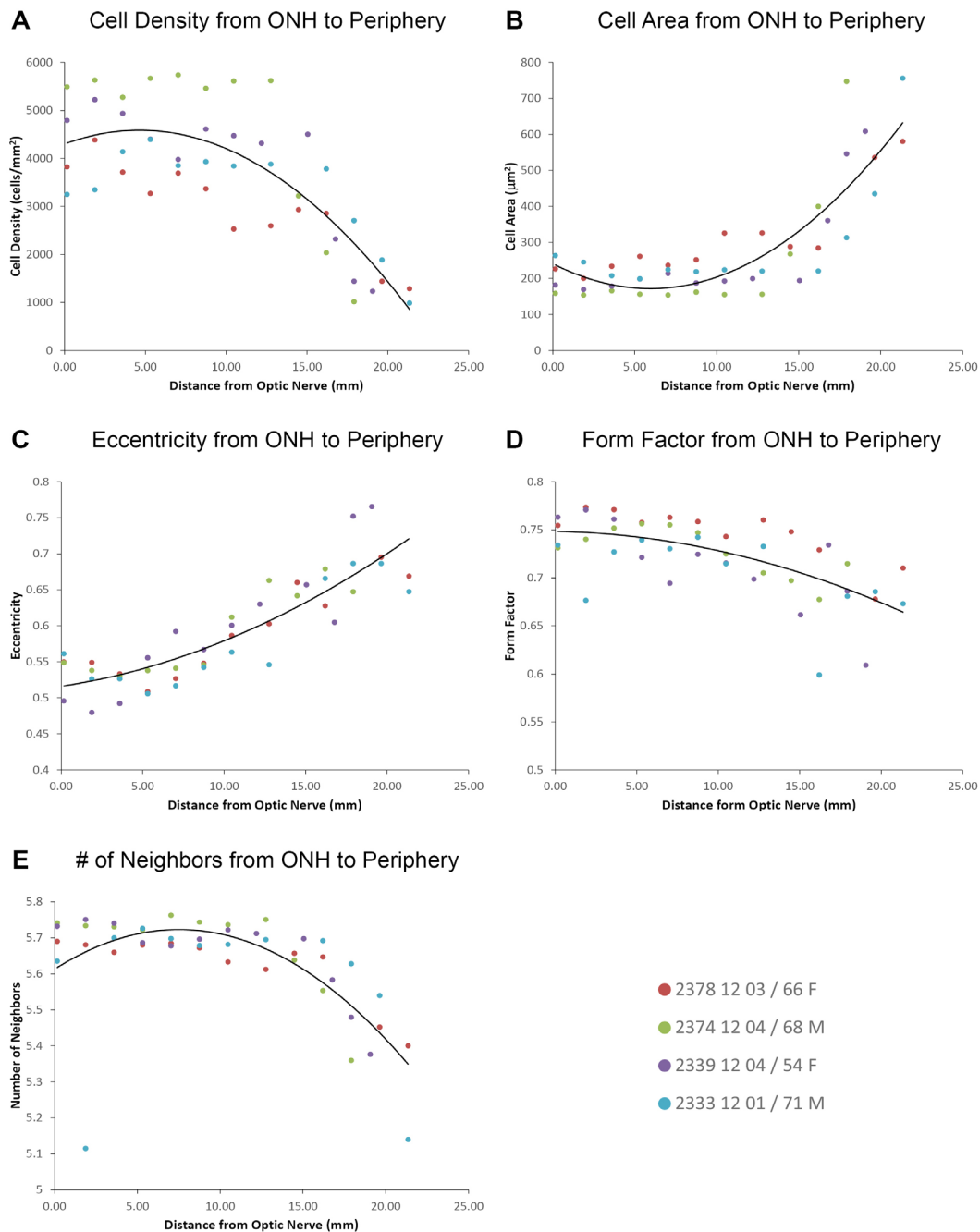
Figure 4. Location study. **A**: Cell density from the optic nerve head (ONH) to the far periphery. Cell density appeared to remain consistent until approximately 13 mm from the optic nerve (i.e., the far periphery). Cell density at the posterior pole was more than four times greater than at the far periphery. **B**: Cell area according to distance from the ONH. The cell area appeared to remain consistent until approximately 15 mm from the optic nerve (i.e., the far periphery). The mean cell areas at the far periphery were almost four times value at the macula/ posterior pole. **C**: Eccentricity varies according to distance from the optic nerve head. There was a clear trend for increasing eccentricity from the macula toward the far periphery. This was the only parameter where the comparison between the macula and the mid-periphery was statistically significantly different. **D**: Form factor variation from the optic nerve head to the far periphery. The highest form factor values were at the macular region, correlating closely to a regular hexagon. Form factor values increased toward the far periphery, revealing the cells became more elongated and asymmetric beyond the posterior pole. **E**: Sidedness varies according to distance from the optic nerve head. The average number of neighboring cells is 5.7 in most series (i.e., about three times as many hexagons as pentagons). We found a trend toward a decrease in sidedness, most pronounced in the far periphery where there were about equal numbers of five- and six-sided RPE cells. The curves on each panel in Figure 4 were created using the trendline tool in Excel and a second-order polynomial for regression. Each trendline was from all four individuals.

TABLE 2. GEOGRAPHIC LOCATION STUDY−CELL DENSITY AS A FUNCTION OF DISTANCE FROM OPTIC NERVE HEAD.

Comparison: Cell density	Mean 1	Mean 2	Mean Diff.	SEM of diff.	n1	n2	q	DF	Significant?	Adjusted P Value
Macula versus Mid Periphery	454	414.5	39.47	53.26	4	4	1.048	9	No	0.7462
Macula versus Far Periphery	454	205.1	248.9	53.26	4	4	6.609	9	Yes	0.003
Mid-Periphery versus Far Periphery	414.5	205.1	209.4	53.26	4	4	5.561	9	Yes	0.0087

1-way ANOVA with Tukey analysis of Cell Density. Geographic spots or locations were defined as follows from left to right as illustrated in Figure 2A— "Macula" represents the first four images, left to right. The "mid–periphery" is defined as Images 5–8. The "Far periphery" represents all the remaining images: 9-through whatever remained. The data suggest that cells in the far periphery were less dense than those in the macula and mid-periphery.

with one central pyknotic cell surrounded by five to six larger cells, which appeared to migrate toward the central cell. These structures are referred to as "cellular rosettes" [27].

Univariate analysis and age: Cell area, measured in (μm)^2, showed a larger coefficient of variation (45%) when compared to cell density (23%), eccentricity (27%), hexagonality (11%), and form factor (11%; Table 8).

Linear regression analysis and age: Linear regression showed a nearly perfect linear correlation between the reciprocal of

the average cell area and cell density ($r^2 = 0.99$; Figure 6A). (We expected a perfect correlation had there been absolutely no gaps between cells or missing cells from the RPE monolayer.) A strong negative correlation was observed between the form factor and the average eccentricity ($r^2 = 0.75$; Figure 6B). A positive correlation was observed between the average cell area and the average eccentricity and between the cell density and the average form factor ($r^2 = 0.70$ and 0.54, respectively; Figure 6C,D). A negative correlation was observed between the cell density and the average eccentricity and between

TABLE 3. GEOGRAPHIC LOCATION STUDY−CELL AREA AS A FUNCTION OF DISTANCE FROM OPTIC NERVE HEAD.

Comparison: Cell Area	Mean 1	Mean 2	Mean Diff.	SEM of diff.	n1	n2	q	DF	Significant?	Adjusted P Value
Macula versus Mid-Periphery	517.6	572.5	−54.91	75.5	4	4	1.029	9	No	0.7541
Macula versus Far-Periphery	517.6	1191	−673.6	75.5	4	4	12.62	9	Yes	<0.0001
Mid Periphery versus Far Periphery	572.5	1191	−618.7	75.5	4	4	11.59	9	Yes	<0.0001

1-way ANOVA with Tukey analysis of Cell Area. Geographic spots or locations were defined as in Figure 2A and Table 2. The data suggest that cells in the far periphery had larger cell areas than those in the macula and mid-periphery.

TABLE 4. GEOGRAPHIC LOCATION STUDY−FORM FACTOR AS A FUNCTION OF DISTANCE FROM OPTIC NERVE HEAD.

Comparison: Form Factor	Mean 1	Mean 2	Mean Diff.	SEM of diff.	n1	n2	q	DF	Significant?	Adjusted P Value
Macula versus Mid-Periphery	0.7455	0.7296	0.01597	0.01403	4	4	1.61	9	No	0.5159
Macula versus Far-Periphery	0.7455	0.6835	0.06205	0.01403	4	4	6.257	9	Yes	0.0042
Mid-Periphery versus Far-Periphery	0.7296	0.6835	0.04608	0.01403	4	4	4.646	9	Yes	0.0232

1-way ANOVA with Tukey analysis of Form Factor. Geographic spots or locations were defined as in Figure 2A and Table 2. The data suggest that cells in the far periphery had reduced form factors than those in the macula and mid-periphery.

TABLE 5. GEOGRAPHIC LOCATION STUDY–ECCENTRICITY AS A FUNCTION OF DISTANCE FROM OPTIC NERVE HEAD.

Comparison: eccentricity	Mean 1	Mean 2	Mean Diff.	SEM of diff.	n1	n2	q	DF	Significant?	Adjusted P Value
Macula versus Mid-Periphery	0.5274	0.5813	−0.05385	0.01396	4	4	5.455	9	Yes	0.0097
Macula versus Far-Periphery	0.5274	0.6733	−0.1459	0.01396	4	4	14.78	9	Yes	<0.0001
Mid-Periphery versus Far-Periphery	0.5813	0.6733	−0.09209	0.01396	4	4	9.327	9	Yes	0.0003

1-way ANOVA with Tukey analysis of eccentricity. Geographic spots or locations were defined as in Figure 2A and Table 2. The data suggest that cells in the far periphery were more eccentric than those in the macula and mid-periphery. Also, cells in the macula were less eccentric than those in the mid-periphery.

TABLE 6. GEOGRAPHIC LOCATION STUDY–POLYGONALITY OF CELLS AS A FUNCTION OF DISTANCE FROM OPTIC NERVE HEAD.

Comparison: Polygonality	Mean 1	Mean 2	Mean Diff.	SEM of diff.	n1	n2	q	DF	Significant?	Adjusted P Value
Macula versus Mid-Periphery	5.67	5.692	−0.02184	0.04011	4	4	0.7701	9	No	0.8518
Macula versus Far-Periphery	5.67	5.497	0.1725	0.04011	4	4	6.084	9	Yes	0.0051
Mid-Periphery versus Far-Periphery	5.692	5.497	0.1944	0.04011	4	4	6.854	9	Yes	0.0024

1-way ANOVA with Tukey analysis of polygonality. Geographic spots or locations were defined as in Figure 2A and Table 2. The data suggest that cells in the far periphery had a slightly reduced number of neighbors than those in the macula and mid-periphery.

the average cell area and the average form factor ($r^2 = 0.62$ and 0.57, respectively; Figure 6E,F). No statistically significant correlations were observed between the percentage of hexagonal cells and the other measures of RPE morphometry ($r^2<0.2$ for all correlations).

Spatial variation of RPE morphometry and age: Average cell density was statistically significantly higher in the macula and the mid-periphery than in the far periphery (Figure 7A). Cell area was statistically significantly greater in the far periphery than in the macula and the mid-periphery (Figure 7B). Eccentricity was statistically significantly greater in

TABLE 7. AGING STUDY DONOR CHARACTERISTICS.

| Age	Race	Sex	Cause of Death	Ocular history	Death to Preservation Time (hours)	# of Eyes Used
29	White	M	Unknown	None noted	Not determined	2
37	White	F	Stroke	Refractive error	0.65	2
42	White	M	GI bleeding	None noted	5.76	1
54	White	F	Ovarian Cancer	None noted	6.53	1
62	White	M	Pancreatic Cancer	None noted	4.80	1
67	White	F	Breast Cancer	None noted	2.95	1
71	White	F	Lung Cancer	Retinal detachment, cataract	6.48	2
71	White	M	Brain Cancer	None noted	3.78	2
75	White	M	Unknown	None noted	3.86	2
80	White	M	Bladder Cancer	None noted	4.00	1
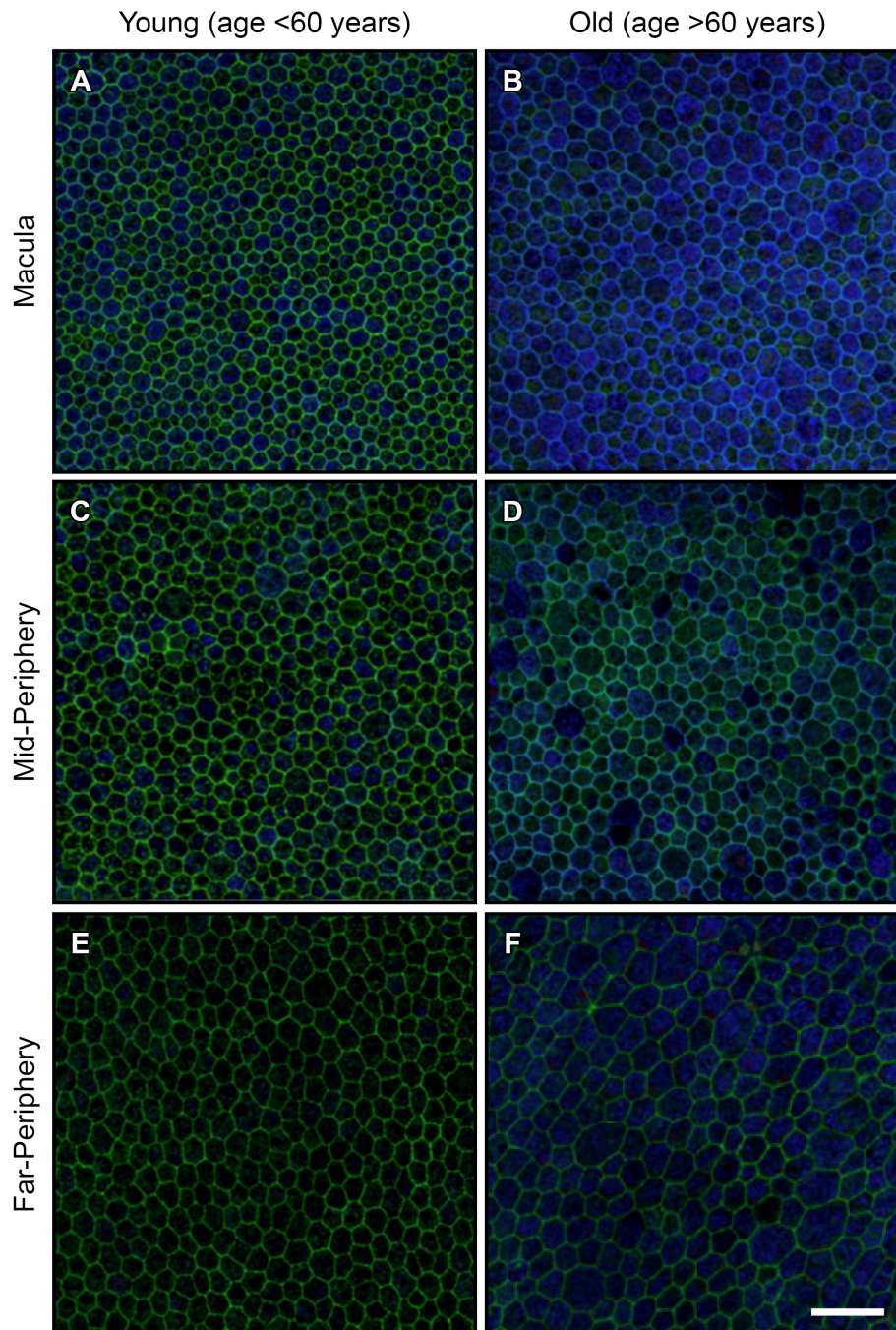
Figure 5. Representative images of RPE flatmounts. Representative images comparing a "young" donor (37 years old; **A**, **C**, and **E**) to an "old" donor (75 year old; **B**, **D**, and **F**) are shown. When qualitatively and subjectively compared to the young donor, the old donor's cells appear to be larger, more elongated, and more variable in area and shape. Scale bar = 50 μm.

the far periphery than in the mid-periphery and the macula. The mid-periphery was in between the macula and the far periphery (Figure 7C). The form factor in the macula and the mid-periphery was greater than in the far periphery (Figure 7D). The macula and the mid-periphery had more neighbors than the far periphery (Figure 7E). The general trend was that

RPE cells in the macula and the mid-periphery were similar in area and shape, while the RPE cells in the far periphery were different, with larger areas and more irregular and varied shapes.

RPE morphology and age: The macula: The average RPE cell density of a 512×512 pixel^2 image in the macula was

TABLE 8. AGING STUDY: DESCRIPTIVE STATISTICS OF RPE MORPHOMETRIC MEASUREMENTS.

Statistic	Macula	Mid-Periphery	Far-Periphery
Cell Density			
Average (SD[1])	4964.52 (1039.55)	3989.53 (521.51)	2521.22 (907.88)
Median (IQR[2])	4966.28 (1184.80)	4176.41 (450.88)	2290.61 (1515.55)
Cell Area			
Average (SD)	177.34 (81.67)	215.39 (88.44)	328.62 (162.82)
Median (IQR)	158.41 (86.93)	197.82 (90.22)	285.91 (176.95)
Eccentricity			
Average (SD)	0.51 (0.16)	0.55 (0.15)	0.63 (0.15)
Median (IQR)	0.50 (0.19)	0.54 (0.20)	0.65 (0.20)
Form Factor			
Average (SD)	0.76 (0.09)	0.75 (0.08)	0.74 (0.08)
Median (IQR)	0.78 (0.07)	0.77 (0.07)	0.76 (0.07)
% Hexagonal Cells			
Average (SD)	40.17 (4.42)	38.51 (3.69)	39.40 (5.00)
Median (IQR)	39.50 (3.71)	38.78 (3.43)	41.24 (4.06)

[1]SD represents standard deviation. [2] IQR represents interquartile range.

4,960±1,040 cells/mm². An overall trend of decreasing RPE cell density with age was observed in the macula (r^2 = 0.32, p = 0.03; Figure 8A). We observed that the rate of decrease in the density of macular RPE cells was 0.54% per year. When the individuals were divided into two age groups, <60 years old and ≥60 years old, there was a higher cell density in the younger group when compared to the older group (Table 9, p = 0.03). The average cell area of an RPE cell in the macula over all ages was 182.1 +/− 86.7 μm². A trend of increasing average cell area with age was observed in the macula (r^2 = 0.34, p = 0.02; Figure 8B). The cell area was also higher in the group with subjects ≥60 years of age (Table 9, p = 0.02). Among all donors, the average percent of hexagonal RPE cells in the macula was 40%. The percent of hexagonal cells showed a decreasing trend with age (r^2 = 0.31, p = 0.03), and when older and younger groups were compared, the percent of hexagonal cells was higher in the younger group (Table 8, p = 0.01; Figure 8C). The average eccentricity of all macular RPE cells was 0.51±0.16. Average eccentricity showed a trend toward a higher value with increasing age (r^2 = 0.48, p = 0.004), and was higher in the older group, signifying that cells had a more elongated shape as they aged (Table 9, p = 0.01; Figure 8D). The average form factor value of the macular RPE cells was 0.76±0.09 and displayed a decreasing trend with age (r^2 = 0.42, p = 0.001) and a lower average value in the older group, indicating that older cells were less symmetric (Table 9, p = 0.03; Figure 8E).

RPE morphology and age: The mid-periphery: The RPE cells of the mid-periphery were examined for age-dependent morphometric changes. Images used for analysis of the RPE of the mid-periphery were selected by measuring approximately 6.2–7.5 mm from the macular region. Fourteen eyes from ten donors of varying ages ranging from 29 to 80 years were used. The average cell density of RPE cells among all ages in a 512 × 512 pixel image of the mid-periphery was 3,990±522 cells/mm². The average area of the RPE cells in the mid-periphery was 215.4±88.4 μm². Among all samples, the average percent of hexagonal cells was 38.51%. The average eccentricity was 0.55±0.15, and the average form factor was 0.75±0.08. There was a weak correlation between the morphometric parameters and age (Figure 8, r^2<0.21 and p>0.05 for all measurements). When the individuals were divided into two age groups, <60 years old and ≥60 years old, there were no statistically significant differences between the younger and older groups in any of the measured morphometric parameters (Table 9, p >0.05 for all measurements).

RPE morphology and age: The far periphery: RPE cells from the far periphery of the retina were analyzed. Images used for analysis of the RPE of the far periphery were selected by measuring a total distance of approximately 13.7 to 16.2 mm from the macular region. Fourteen eyes from nine donors of varying ages ranging from 29 to 80 years old were used. The average RPE cell density of a 512 × 512 pixel² image in the far periphery was 2,520±908 cells/mm². An overall
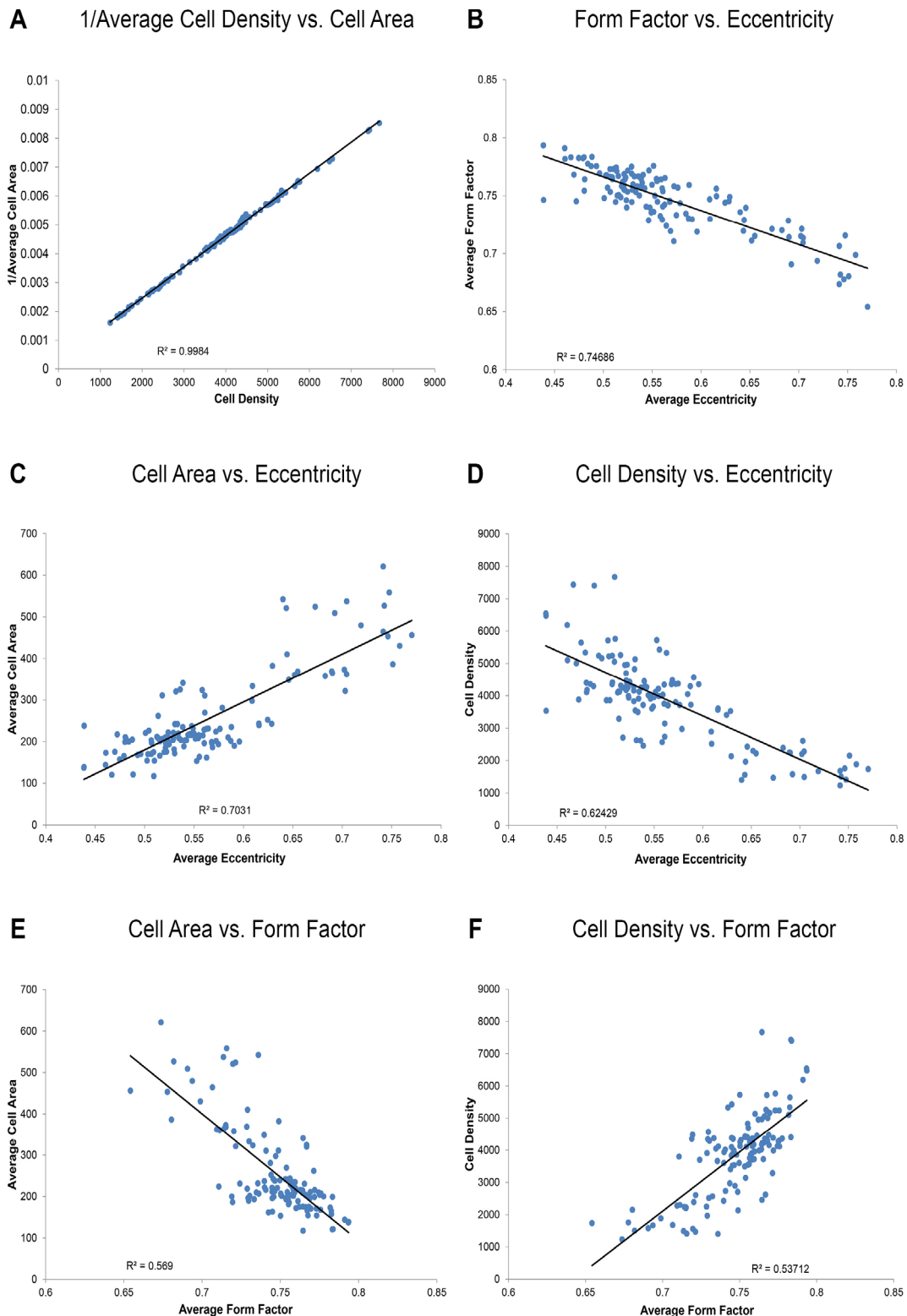
Figure 6. Correlation analysis. **A**: There is a perfect correlation between the reciprocal of the average cell area and cell density (because there were no extracellular gaps, spaces, or atrophic regions between cells). **B**: There is a strong negative correlation between average form factor and average eccentricity, confirming integrity of our data set. **C**: There were positive correlations between the average cell area and average eccentricity. **D**: There were positive correlations between cell density and average form factor. **E**: Negative correlations exist between the average cell area and the form factor. **F**: Negative correlations exist between the cell density and average eccentricity.
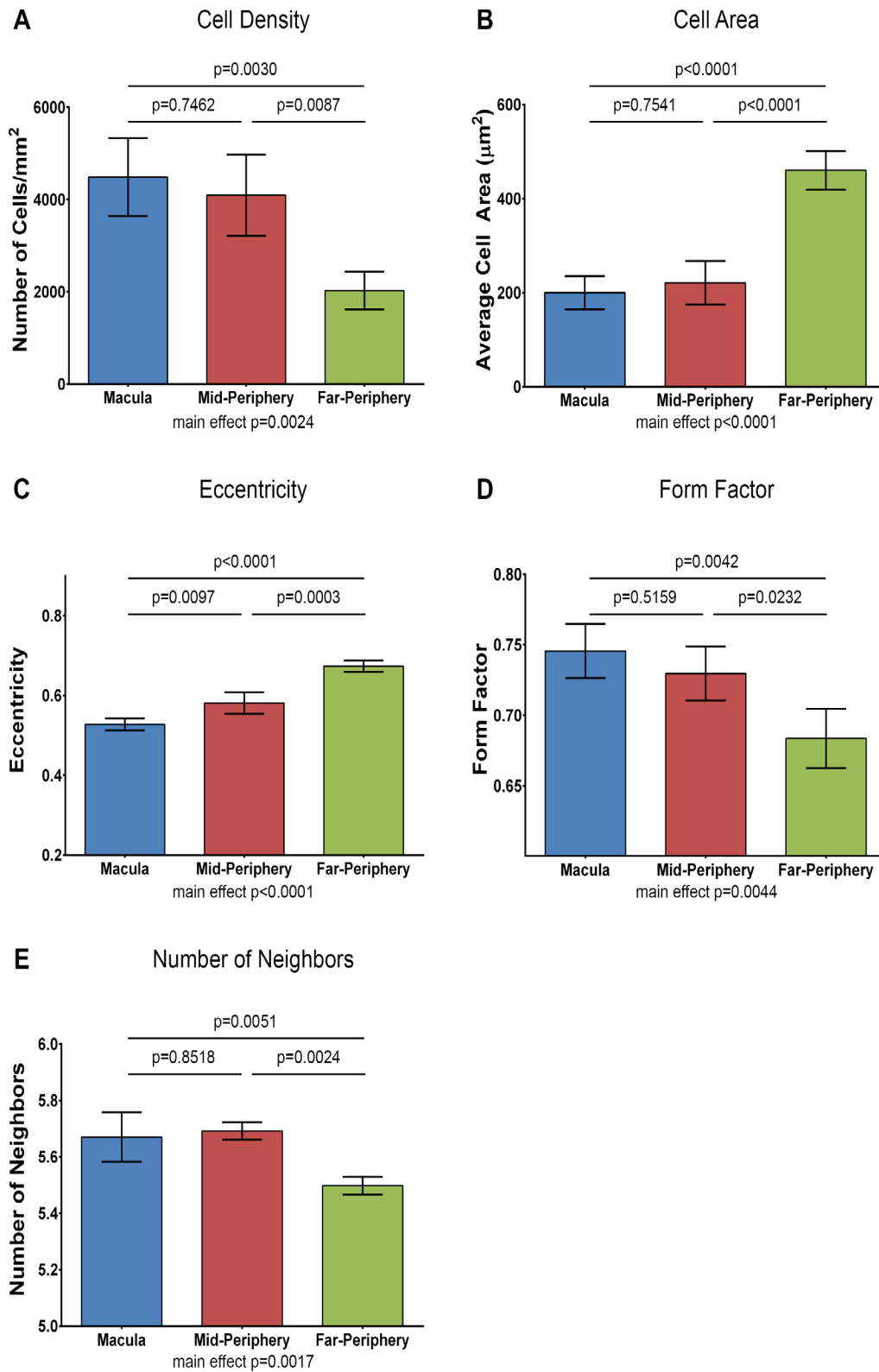
Figure 7. Analysis of spatial variation of RPE morphometry. **A**: Average cell density. **B**: Average cell area. **C**: Average eccentricity. **D**: Average form factor. **E**: Average percentage of hexagonal cells. These were averaged across all age groups in three areas of the retina. Error bars represent standard deviations. One-way ANOVA with Tukey's multiple comparisons test. P values are provided on the image. RPE cells in the macula and the mid-periphery were generally similar in area and shape while the far periphery differed with larger areas of more irregularly shaped RPE cells.
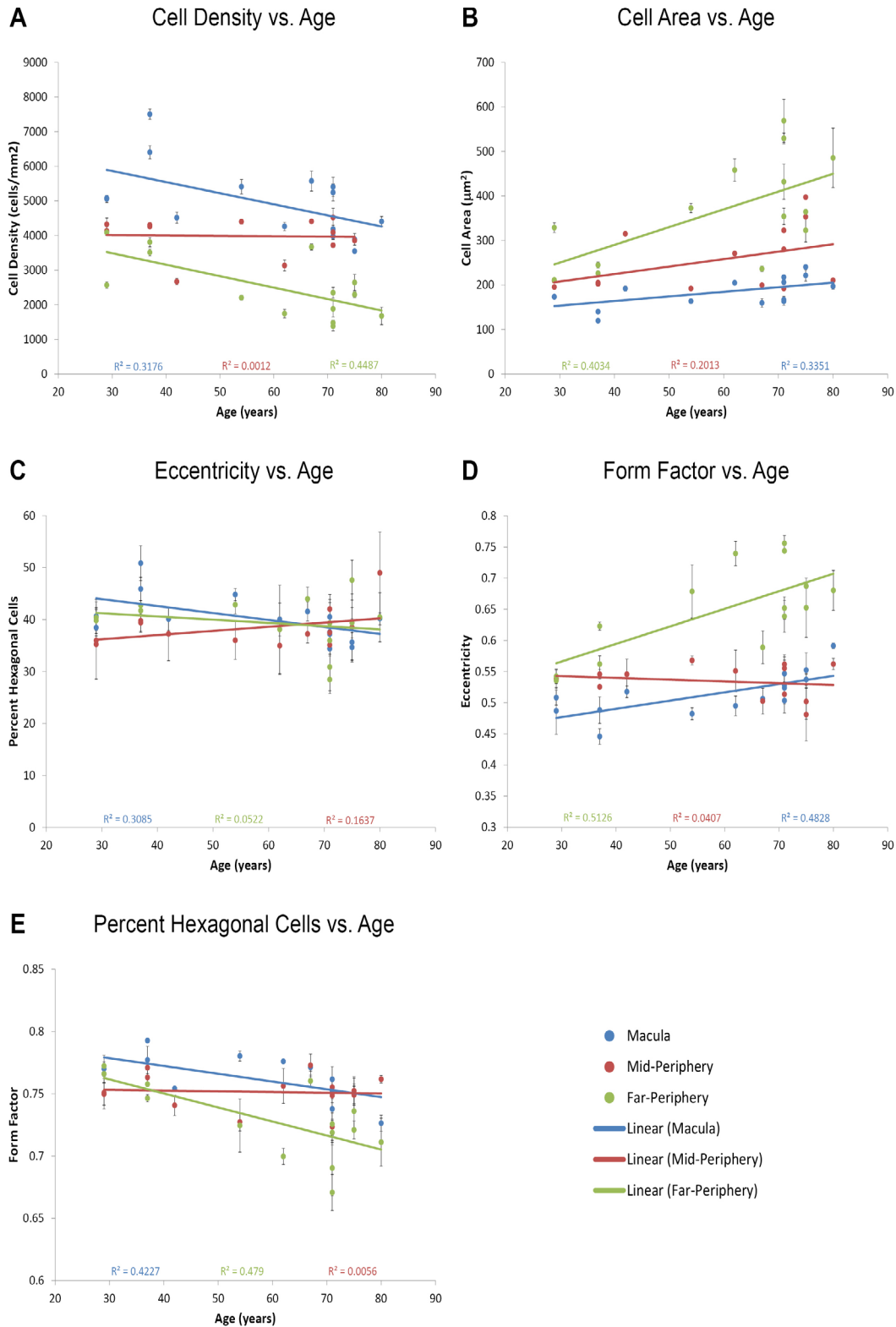
Figure 8. Composite graphs showing age-related morphometric alterations in the RPE in all three areas of the retina. Various morphometric measurements from three areas of the retina are plotted against age. In general, the mid-periphery was resistant to change over age, while the macula and the far periphery showed similar trends in changes with age in all metrics except eccentricity. **A**: Cell density. **B**: Cell area. **C**: eccentricity. **D**: Form factor. **E**: Percentage of hexagonal cells. Each point on the graph represents an average of measurements taken from three images from a single donor. The error bars represent the standard deviation of those three measurements.

trend of decreasing RPE cell density with age was seen in the far periphery ($r^2 = 0.45$, p = 0.001; Figure 8A). We observed that the rate of decrease in the density of RPE cells in the far periphery was 0.94% per year. When individuals were divided into two age groups, <60 years old and ≥60 years old, there was higher cell density in the younger group (Table 9, p = 0.02). The average cell area for the RPE cells in the far periphery was 329±163 μm^2. A trend of increasing average cell area with age was observed in the far periphery ($r^2 = 0.40$, p = 0.01; Figure 8B). The cell area was larger in the older group (Table 9, p = 0.02). Among all samples, the average percent of hexagonal RPE cells in the far periphery was 39.40%. The percent of hexagonal cells showed a minimal association with age ($r^2 = 0.05$, p = 0.43), and when older and younger groups were compared, the percent of hexagonal cells was not statistically significantly different than in the younger group (Table 9, p = 0.26; Figure 8C). The average eccentricity of RPE cells in the far periphery was 0.63±0.05. The average eccentricity showed a trend toward a higher value and a more elongated shape with age ($r^2 = 0.51$, p = 0.004) and was higher in the older group (Table 9, p = 0.01; Figure 8D). The form factor had an average value of 0.74±0.08 and displayed a decreasing trend with age ($r^2 = 0.48$, p = 0.006) and a lower average value in the older group (Table 9, p = 0.01; Figure 8E).

DISCUSSION

Normal area and shape of RPE cells: Studies such as this are limited by the availability of human cadaver eyes. In the future, we expect much larger data sets obtained by routine noninvasive imaging instruments that are currently approaching the commercial market. These future instruments will allow populations to be characterized with appropriate genetics and clinical phenotyping that will compensate for high subject-to-subject variability. A key point of this study is that it provides baseline information about subject-to-subject variability for rigorous power analysis of sample size for future studies. We found that there are differences in RPE cell area and shape characteristics between age groups in some regions of the retina but not in other regions. This finding substantiates several of our posited expectations and the quantitative objective approach.

Location characteristics of healthy RPE: Depending on location, we found statistically significant spatial differences in RPE cell density. Cell area also varied by location. Cell density and cell area were closely related inversely, because there were only rare and small gaps in the RPE sheet regardless of age in the normal eyes. This inverse relationship is clearly broken when large gaps in the sheet appear, for example, in geographic atrophy. In agreement with previous

Region	Measurement	Average <60 years	Average ≥60 years	p-value*
Macula				
	Cell Density	5662.35	4499.31	**0.03**
	Cell Area	160.37	197.48	**0.02**
	Eccentricity	0.49	0.5315	**0.01**
	Form Factor	0.77	0.7528	**0.03**
	% Hexagonal Cells	43.46	37.98	**0.01**
Mid-Periphery				
	Cell Density	4014.60	3823.90	0.57
	Cell Area	219.93	219.47	0.98
	Eccentricity	0.54	0.53	0.36
	Form Factor	0.75	0.75	0.78
	% Hexagonal Cells	37.278	39.33	0.30
Far-Periphery				
	Cell Density	3235.82	2124.23	**0.02**
	Cell Area	276.74	416.80	**0.02**
	Eccentricity	0.59	0.6821	**0.01**
	Form Factor	0.75	0.7149	**0.01**
	% Hexagonal Cells	41.50	38.24	0.26

TABLE 9. AGING STUDY: AVERAGE MORPHOMETRIC MEASUREMENTS COMPARING PATIENTS <60 YEARS AND ≥60 YEARS OF AGE.

* α=0.05, significant p values marked in **bold**

studies, we observed that RPE cells became less dense and larger with increasing distance from the optic nerve [5]. Cell density was consistently statistically significantly higher at the macula compared to the temporal periphery (p<0.05), with a marked change approximately two-thirds of the distance from the ONH to the temporal far periphery. RPE cells in the macular region had a regular, predominantly hexagonal shape, with the RPE maintaining this structure in the mid-periphery despite the increasing cell area. The far periphery had marked irregularity and variation in RPE cell shape and area, and the difference from the macula to the periphery was statistically significant for all three measures (p<0.05), based on the eccentricity, form factor, and topology measurements. For all parameters, a clear trend was seen from the macula to the periphery. The regular shape of the cells in the macular region suggests that there are no external forces causing irregular tension. However, the peripheral RPE cells were more irregular in shape and area, suggesting that there are forces causing irregular tension on the cells in that location. The higher density of RPE cells in the macular and mid-peripheral regions may be necessary to support the requirements of the retina and increased cone density there. It is also possible that the high cell density in the mid-periphery serves as a zone of cells that can migrate to replenish dying cells in the macula.

The finding that RPE cell density decreases with increasing distance from the optic nerve confirms and extends the findings of Gao and Hollyfield [11], Panda-Jonas et al. [5], and Del Priore et al. [6]. Gao and Hollyfield [11] showed foveal RPE cell density is 63% higher than in the periphery, while the present study showed the macular RPE cell density is about 97% higher than in the periphery. As in the present study, Panda-Jonas et al. [5] and Del Priore et al. [6] quantified RPE cell density in various areas of the retina. Del Priore et al. [6] showed macular RPE cell density is 4,980±90 cells/mm^2, which is similar to the present finding of 4,960±1040 cells/mm^2.

The substantial variability in the data reported in the literature can be partly explained by differences in the methods used among investigators to sample various areas of the retina. Furthermore, there can be great variability within a study, emphasizing the importance of sampling the same location relative to the optic nerve in each eye, as noted by Watzke et al. [7]: We avoided this variability by sampling the same locations (relative to the ONH) across subjects. Many of the previous studies also measured RPE cell density by simply counting the number of stained nuclei present. This method can be inaccurate and falsely overestimate cell density, because we observed in our images (as have

others; Starnes et al., IOVS 2015; 56: ARVO E-Abstract 2371) that many RPE cells are multinucleate. For this reason, we assessed cell density by automatically outlining cell borders and counting whole cells, instead of nuclei.

Additionally, many earlier studies used sectioned or bleached tissues for their analyses, yielding low-quality images to obtain cell counts. In several recent studies, RPE cells have been imaged with greater resolution due to improvements in imaging techniques. The present study is the first to use imaging analyses and results that are clinically translatable and automated. We imaged RPE cells using confocal microscopy, an imaging technique that provides high-resolution images of RPE cells. AOSLO technology now provides images of the RPE sheet approaching that which can be analyzed by the same metrics, in vivo and non-invasively [28].

One limitation of the present study was that only RPE cells from the temporal macula and temporal periphery were sampled. RPE cells from the nasal retina were not included in the tissue that was analyzed. Because RPE cells likely differ based on their location in the retina, we hope to include additional topological areas of the retina in future studies.

Aging of the RPE: Although age-related loss of RPE cells has been reported in the literature, to our knowledge the details surrounding exactly how the shape of RPE cells changed with age have not been investigated. The present study confirms the conclusions of previous investigations that there is an overall age-related decline in RPE cell density. We found a 0.45% decrease in overall RPE cell density per year, a slightly higher rate of decline than the previous findings of Panda-Jonas et al. [5] and Del Priore et al. [6], who found a 0.3% and 0.23% rate of decline per year, respectively (Table 1). Although most previous studies looked at small portions of the retina, the present study investigated RPE cell morphometry from a continuous strip of tissue that included three zones of the retina: the macula, mid-periphery, and far periphery. The findings that RPE cell density in the macula decreases with age confirms previous studies by Ts'o and Friedman [9], and Dorey et al. [10]. However, in contrast to these two studies, we found a statistically significant decrease in RPE cell density with age in the peripheral retina as well. We found that the average rate of peripheral RPE cell loss was about 32 cells/mm^2 per year, while Gao and Hollyfield [11] reported a lower rate of decline at 14 RPE cells/mm^2 per year.

The present study showed that RPE cell morphometry changes with age in the macula and the temporal far periphery but not in the temporal mid-periphery. We concluded that RPE cells in the macula and the far periphery become less numerous, larger, more elongated, and less

hexagonal with increasing age. These changes may have been observed in the macula because there may be the greatest cell loss in this area of the retina. The macula is highly metabolically active, which may cause a buildup of toxic waste over time. With increasing age, this toxic burden eventually may become excessive, leading to age-related changes [7]. These changes can damage the integrity of RPE cells over time and ultimately lead to cell death [29]. The temporal mid-periphery of the retina, however, seems to be protected from these age-related changes perhaps because this region is a generally stable area of the retina where less general damage occurs [30]. In addition, RPE cell migration of peripheral RPE cells may help compensate for the death of cells in the mid-periphery, masking any age-related changes. The far periphery of the retina shows age-related changes in RPE morphometry possibly caused by retinal and RPE thinning that may be worsened with increasing age [29]. It is also thought that the far periphery may be more likely to be remodeled because of the presence of RPE stem cells in the marginal zone region of the ciliary body of some species [31].

The present findings suggest that with the gradual loss of RPE cells, existing RPE cells become larger to fill in the empty spaces left behind by dying cells. This mechanism preserves the overall stability and integrity of the RPE monolayer as found in chick RPE [32]. We observed numerous manifestations of this process in the form of cellular rosettes (Figure 5, bottom right image). These clusters of cells appeared as one central pyknotic cell surrounded by five to six larger cells, which were migrating toward the central cell. The surrounding cells appeared to be more stretched and elongated, explaining our observation of increased average cellular eccentricity with older age [27]. Prompt detection of these structures may serve as an early diagnostic method for retinal pathologies that involve RPE cell death.

Age-dependent changes were observed in the RPE morphometry of the normal aging eye. With age, RPE cells from the macula, on average, become larger and more elongated. These observed differences in the aging eye may resemble early changes seen in the pathologic changes in the RPE as may occur in AMD. This study showed that changes seen with age and location of the retina can be visibly detected; these findings may provide a baseline for normal RPE morphometric aging in these images. Data from this study can be used to detect individuals who are outside the normal range, and possibly considered for treatments [33].

REFERENCES

1. Ehrlich R, Harris A, Kheradiya NS, Winston DM, Ciulla TA, Wirostko B. Age-related macular degeneration and the aging eye. Clin Interv Aging 2008; 3:473-82. [PMID: 18982917].

2. Liang F-Q, Godley BF. Oxidative stress-induced mitochondrial DNA damage in human retinal pigment epithelial cells: a possible mechanism for RPE aging and age-related macular degeneration. Exp Eye Res 2003; 76:397-403. [PMID: 12634104].

3. Foulds WS. The retinal-pigment epithelial interface. Br J Ophthalmol 1979; 63:71-84. [PMID: 427074].

4. Thompson DW. On growth and form. Cambridge, UK: 1942

5. Panda-Jonas S, Jonas JB, Jakobczyk-Zmija M. Retinal pigment epithelial cell count, distribution, and correlations in normal human eyes. Am J Ophthalmol 1996; 121:181-9. [PMID: 8623888].

6. Del Priore LV, Kuo Y-H, Tezel TH. Age-related changes in human RPE cell density and apoptosis proportion in situ. Investigative Ophthalmology &amp Visual Science 2002; 43:3312-8.

7. Watzke RC, Soldevilla JD, Trune DR. Morphometric analysis of human retinal pigment epithelium: correlation with age and location. Curr Eye Res 1993; 12:133-42. [PMID: 8449024].

8. Harman AM, Fleming PA, Hoskins RV, Moore SR. Development and aging of cell topography in the human retinal pigment epithelium. Investigative Ophthalmology &amp Visual Science 1997; 38:2016-26.

9. Tso MO, Friedman E. The retinal pigment epithelium. 3. Growth and development. Arch Ophthalmol 1968; 80:214-6. [PMID: 5661888].

10. Dorey CK, Wu G, Ebenstein D, Garsd A, Weiter JJ. Cell loss in the aging retina. Relationship to lipofuscin accumulation and macular degeneration. Investigative Ophthalmology &amp Visual Science 1989; 30:1691-9.

11. Gao H, Hollyfield JG. Aging of the human retina. Differential loss of neurons and retinal pigment epithelial cells. Investigative Ophthalmology &amp Visual Science 1992; 33:1-17.

12. Roorda A. Applications of adaptive optics scanning laser ophthalmoscopy. Optom Vis Sci 2010; 87:260-8. [PMID: 20160657].

13. Morgan JIW, Dubra A, Wolfe R, Merigan WH, Williams DR. In vivo autofluorescence imaging of the human and macaque retinal pigment epithelial cell mosaic. Investigative Ophthalmology &amp Visual Science 2009; 50:1350-9.

14. Roorda A, Zhang Y, Duncan JL. High-resolution in vivo imaging of the RPE mosaic in eyes with retinal disease. Investigative Ophthalmology &amp Visual Science 2007; 48:2297-303.

15. McCarey BE, Edelhauser HF, Lynn MJ. Review of corneal endothelial specular microscopy for FDA clinical trials of refractive procedures, surgical devices, and new intra-ocular drugs and solutions. Cornea 2008; 27:1-16. [PMID: 18245960].

16. Heron M. Deaths: leading causes for 2010. National vital statistics reports: from the Centers for Disease Control and Prevention, National Center for Health Statistics National Vital Statistics System 2013; 62:1-96.

17. Huang JC, Voaden MJ, Zarbin MA, Marshall J. Morphologic preservation and variability of human donor retina. Curr Eye Res 2000; 20:231-41. [PMID: 10694900].

18. Van Meter WS, Katz DG, White H, Gayheart R. Effect of death-to-preservation time on donor corneal epithelium. Trans Am Ophthalmol Soc 2005; 103:209-2.

19. Schneider CA, Rasband WS, Eliceiri KW. NIH Image to ImageJ: 25 years of image analysis. Nat Methods 2012; 9:671-5. [PMID: 22930834].

20. Linkert M, Rueden CT, Allan C, Burel J-M, Moore W, Patterson A, Loranger B, Moore J, Neves C, Macdonald D, Tarkowska A, Sticco C, Hill E, Rossner M, Eliceiri KW, Swedlow JR. Metadata matters: access to image data in the real world. J Cell Biol 2010; 189:777-82. [PMID: 20513764].

21. Carpenter AE, Jones TR, Lamprecht MR, Clarke C, Kang IH, Friman O, Guertin DA, Chang JH, Lindquist RA, Moffat J, Golland P, Sabatini DM. CellProfiler: image analysis software for identifying and quantifying cell phenotypes. Genome Biol 2006; 7:R100-[PMID: 17076895].

22. Chrenek MA, Dalal N, Gardner C, Grossniklaus H, Jiang Y, Boatright JH, Nickerson JM. Analysis of the RPE sheet in the rd10 retinal degeneration model. Adv Exp Med Biol 2012; 723:641-7. [PMID: 22183388].

23. Jiang Y, Qi X, Chrenek MA, Gardner C, Dalal N, Boatright JH, Grossniklaus HE, Nickerson JM. Analysis of Mouse RPE Sheet Morphology Gives Discriminatory Categories. Vol 801. New York, NY: Springer New York; 2014. p. 601–7.

24. Boatright JH, Dalal N, Chrenek MA, Gardner C, Ziesel A, Jiang Y, Grossniklaus HE, Nickerson JM. Methodologies for analysis of patterning in the mouse RPE sheet. Mol Vis 2015; 21:40-60. [PMID: 25593512].

25. William Tasman EJ. Duane's Ophthalmology on CD-ROM: Lippincott Williams & Wilkins; 2013.

26. Doughty MJ. Concerning the symmetry of the 'hexagonal' cells of the corneal endothelium. Exp Eye Res 1992; 55:145-54. [PMID: 1397122].

27. Nagai H, Kalnins VI. Normally occurring loss of single cells and repair of resulting defects in retinal pigment epithelium in situ. Exp Eye Res 1996; 62:55-61. [PMID: 8674513].

28. Rossi EA, Rangel-Fonseca P, Parkins K, Fischer W, Latchney LR, Folwell MA, Williams DR, Dubra A, Chung MM. In vivo imaging of retinal pigment epithelium cells in age related macular degeneration. Biomed Opt Express 2013; 4:2527-39. [PMID: 24298413].

29. de Jong PTVM. Age-related macular degeneration. N Engl J Med 2006; 355:1474-85. [PMID: 17021323].

30. Beatty S, Koh H, Phil M, Henson D, Boulton M. The role of oxidative stress in the pathogenesis of age-related macular degeneration. Surv Ophthalmol 2000; 45:115-34. [PMID: 11033038].

31. Perron M, Harris WA. Retinal stem cells in vertebrates. Bioessays 2000; 22:685-8.

32. Nagai H. KALNINS VI. Normally occurring loss of single cells and repair of resulting defects in retinal pigment epithelium in situ. Exp Eye Res 1996; 62:55-61. [PMID: 8674513].

33. Chew EY, Lindblad AS, Clemons T. Group A-REDSR. Summary results and recommendations from the age-related eye disease study. Arch Ophthalmol 2009; 127:1678-9. [PMID: 20008727].